An empirical study on optical flow accuracy depending on vehicle speed

Naveen Onkarappa and Angel D. Sappa
Computer Vision Center
Autonomous University of Barcelona
Edifici O, 08193 Bellaterra, Barcelona, Spain
{naveen, asappa}@cvc.uab.es

***Abstract*— Driver assistance and safety systems are getting attention nowadays towards automatic navigation and safety. Optical flow as a motion estimation technique has got major roll in making these systems a reality. Towards this, in the current paper, the suitability of polar representation for optical flow estimation in such systems is demonstrated. Furthermore, the influence of individual regularization terms on the accuracy of optical flow on image sequences of different speeds is empirically evaluated. Also a new synthetic dataset of image sequences with different speeds is generated along with the ground-truth optical flow.**

I. INTRODUCTION

Advanced driver assistance systems (ADAS) can benefit in many ways from the visual motion information for applications such as 3D reconstruction, moving object detection, egomotion estimation, autonomous navigation, etc. The well known apparent motion estimation tool is optical flow. It is the two-dimensional vector field of the displacement information for each pixel in the image. The research on optical flow started long back, the seminal approaches [1] and [2] were proposed in 1981. It has got much attention again the last decade. Several approaches have been proposed in the literature to estimate the optical flow. They can be majorly classified into local or global methods. Local methods [2] give sparse flow fields, whereas global approaches [1] give dense flow fields. Here our interest is on global approaches that give dense flow fields even in the absence of enough information in some image regions. Typically, the global methods are formulated as an energy minimization problem that considers the energy in the whole image. The energy function contains a data term which matches some properties in one image with the other image; and a regularization term to make the problem well posed. The first global approach formulated as a variational energy minimization is proposed in [1].

An overview of the developments upto the times can be found in [4] and [5]. In [4], an empirical evaluation of the performance of optical flow algorithms on complex image sequences is presented. Galvin et al. [6] evaluate eight different optical flow algorithms. Recently, McCane et al. [7] proposed a benchmarking set of image sequences and tools for the purpose of evaluating optical flow algorithms. A major obstacle in performing any empirical study in computer vision is obtaining ground truth data. Baker et al. [8] has recently proposed few sequences with ground-truth and an evaluation methodology.

There have been many attempts to improve the accuracy of global optical flow methods (e.g., [15], [16]) since the proposal of seminal methods. Attempts have been done to improve the data term [13], the regularization term (e.g., [11], [12], [14]), the objective function itself, and also the way of minimization. In [5], a detailed overview of the developments in the respective parts of optical flow is given. A recent paper [3] explores concepts such as pre-processing, coarse-to-fine warping, graduated non-convexity, interpolation, derivatives, robustness of penalty functions and median filtering. In [3], an improved model underlying a weighted non-local term based median filtering is proposed. Recently, temporal coherence is incorporated in the flow estimation [10]. Efforts to combine both local and global methods [9] are also made. In such efforts, the advantages from both approaches are combined resulting in more accurate optical flow. Unlike optical flow estimation on traditional datasets, an approach for optical flow estimation of specular dataset is proposed in [17]. Also an effort to represent flow field in polar space is made in [18].

Despite the volume of research on the topic of optical flow, little work has been done looking for the most efficient way to combine data and regularization term. Since the regularization term plays a major role in optical flow computation, there are lot of works proposing different regularization functions, but it is not clear how to find the right balance between data term and the regularization term. Up to our knowledge, almost no attempt has been done to tune the weight of the regularization term based on the properties of the image sequence. The weight of the regularization term is being set empirically for the minimal error.

The work in this paper is motivated by the adaptation of the weight of the regularization term according to some feature of the given sequence, specifically the speed in the image sequence captured by a vehicle camera. Our work empirically analyzes the variation in accuracy of the flow field to the variations in weights of the regularization terms in the polar representation. The influence of different regularization terms is also analyzed. Also new synthetic image sequences with ground-truth optical flow are generated and an evaluation framework using these synthetic scenarios is presented.

The current paper is organized as follows. First, a polar representation of flow vectors is explored in contrast to the cartesian representation, and its suitability to ADAS

domain is discussed in section II. Next, an overview of polar represented optical flow estimation is presented in section III. The generation of image sequences and corresponding ground-truth flow fields are detailed in section IV. The empirical analysis and discussion are presented in section V. Finally, the paper is concluded in Section VI.

II. POLAR VERSUS CARTESIAN IN THE ADAS FIELD

The natural representation of a vector is by its magnitude and orientation. As presented in [18], the two polar components show significant statistical difference compared to two cartesian components, when their spatial derivatives distribution from a flow field is analyzed. Also, two polar components show more statistical independence among them when mutual information between derivatives of the components are analyzed and compared to the mutual information of cartesian components in [18] and [19]. We follow previous studies using synthetic sequences of urban road scenarios (see Fig. 2) when cartesian and polar representations are used to depict motion information. Figure 1 shows joint histograms of flow derivatives in cartesian and polar coordinates. These joint histograms are then used for computing the mutual information (MI) between the coordinate components. Small values of MI indicate more statistical independence. Hence, as shown in Fig. 1 (see MI at the top of every illustration), it can be concluded that, it is more appropriate to represent the flow field in a polar coordinate system.

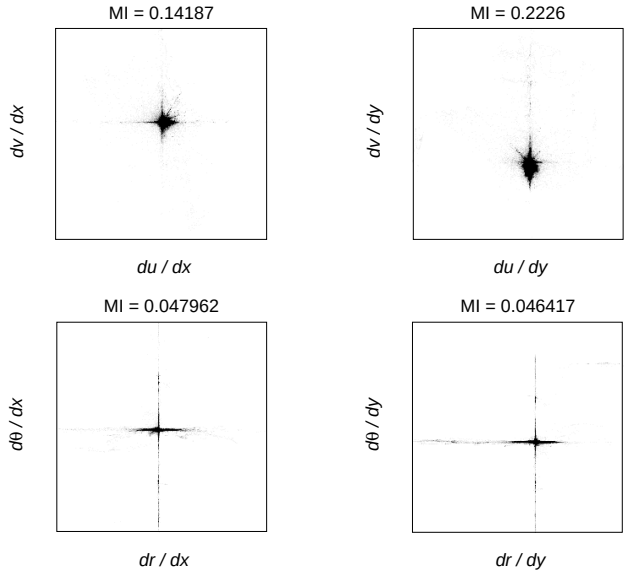

Fig. 1. Joint histograms of flow derivatives in cartesian and polar coordinates of a synthetic sequence of an urban road scenario. On top of each figure MI value is depicted.

In [19], a polar representation of flow vectors in optical flow estimation is proposed and its implications are also studied. The authors claim that flow fields obtained by a polar representation are as accurate as those obtained by the state of the art approaches using a cartesian representation, when evaluated on traditional datasets. As an advantage of polar representation, they also proposed a way of regularizing the different axes independently. This optical flow formulation can be adopted to suit different kinds of datasets such as specular and fluid flow datasets. In the context of vehicle driving, the motion of vehicle camera mainly involves translation along the optical axis considering the camera is forward faced. On these kinds of scenarios, the computed flow fields are divergent. If we assume pure translation, then the orientation of the flow vectors vary less compared to the magnitude, that vary much depending on the speed of the vehicle. Hence, it is intuitive that the polar optical flow method suits well for the context of ADAS.

III. OVERVIEW OF POLAR OPTICAL FLOW

The basic variational formulation of optical flow proposed by Horn and Schunck [1] is given by:

$$E(u,\, v) = \int\int_{\Omega} \{\underbrace{(I(x+u, y+v, t+1) - I(x,y,t))}_{Data\ Term} + \alpha\, (\underbrace{|\nabla u_1|^2 + |\nabla u_2|^2}_{Regularization})\}\, dx\, dy \quad (1)$$

where the energy function is minimized for the flow vectors (u, v). The pixel $(x, y) \in \Omega$ in time t is represented by the intensity $I(x, y, t)$. And α is a factor that weights the regularization term. The data term is the brightness constancy assumption and the smoothness term assumes the estimated flow field varies smoothly all over the image. The energy function can be minimized by applying Euler-Lagrange equations [16] or alternative methods [15].

As discussed in section II about the polar representation, [18] proposes to represent a vector in polar form as:

$$flow(x, y) = (m(x, y), \theta(x, y)) \quad (2)$$

where $m(x, y)$ denotes the magnitude and $\theta(x, y)$ denotes the orientation of the flow vector.

Now the energy function with this notation can be written as:

$$E(\theta(x,y), m(x,y)) = \int\int_{\Omega} \{\psi(I(x + m\cos\theta, y + m\sin\theta, t+1) - I(x,y,t)) + \alpha_\theta \psi_\theta(\rho_\theta(\theta)) + \alpha_m \psi_m(\rho_m(m))\ \}\, dx\, dy \quad (3)$$

where ψ_θ and ψ_m are robust penalty functions; ρ_θ and ρ_m are differential operators, normally the gradients; α_θ and α_m are regularization weighting parameters separately for θ and m components. It is clear from this formulation that the two flow components can be handled independently.

To avoid the problems due to the periodic nature of θ, we can define new variables:

$$s(x, y) = \sin\theta(x, y) \quad (4)$$
$$c(x, y) = \cos\theta(x, y)$$

subject to $s^2 + c^2 = 1$ which is called coherence constraint. With this modification, the energy function can be formulated to minimize three parameters (c, s, m) as:

$$E(c,s,m) = \int\int_{\Omega} \{\ \lambda(s^2+c^2-1)^2 \qquad (5)$$
$$+\psi(I(x+m\cos\theta, y+m\sin\theta, t+1) - I(x,y,t))$$
$$+\ \alpha_\theta \psi_\theta(\rho_\theta(c), \rho_\theta(s)) + \alpha_m \psi_m(\rho_m(m))\ \}\ dx\ dy$$

where λ is a Lagrange multiplier set to $\lambda = e^{(s^2+c^2-1)^2}$ updated before each iteration of the minimization process. Eq. 5 is the final polar optical flow model and it is minimized using Euler-Lagrange equations to obtain the optical flow, more details can be found in [18]. One can notice that Eq. 5 contains two regularization terms for two polar coordinate components, those can be weighted independently.

IV. SYNTHETIC DATASET GENERATION

The goal of this work is to study the adaptation of regularization parameters in optical flow computation for the varying speeds of the moving camera. The requirement is to have several image sequences of the similar scene, but with different speeds of the camera. It is not possible to create the ground-truth optical flow for real sequences, unless performed in a controlled environment. The other option is to create synthetic image sequences with different camera speeds and to generate ground-truth optical flow from the 3D models. There are few available synthetic sequences (e.g., [7] and [8] for general purposes, and [21] for ADAS). But none of them suits our intended study. So, in this section the process of obtaining the dataset with ground-truth optical flow is detailed.

First, the 3D model is constructed using Maya[1]. The constructed model is a typical urban scenario that consists of a straight road with buildings on both sides with appropriate textures. The model does not contain any nurb surfaces nor any moving objects in the scene. The camera is assumed as it is in a car moving in the scene along the straight road. Different image sequences were generated by changing the speed of the camera in the model. The image sequences of different speeds having translation of 0.25cm, 0.5cm, 0.75cm, and 1cm per frame along the optical axis are generated. From now on these sequences are referred to as S1, S2, S3 and S4 in the increasing order of the speed. The images in these sequences are of resolution 640×480 and are rendered using Maya software. Next the ground-truth flow fields are generated by raytracing using the code from [20]. Some images from all these different sequences are shown in Fig. 2. The image in $top-left$ is the common starting frame in all sequences. $top-right$ is the color-map used in this paper to represent the flow fields. $2nd\ row-left$ is the second frame in S1. $3rd\ row-left$ is the second frame in S2 and so on. $right-column$ shows the ground-truth flow fields between the corresponding pairs of all sequences.

The ground-truth flow fields look diverging, the vectors originated from a vanishing point at the center and directed outwards in all direction. One can observe that the black region in the bottom of the flow fields in Fig. 2 is increasing as the speed of the camera increases; this indicates the increase in displacements with increase in speed of sequences. The ground-truth flow vectors are not generated at these black pixels, as those pixels present in the first frame do not exist in the second frame.

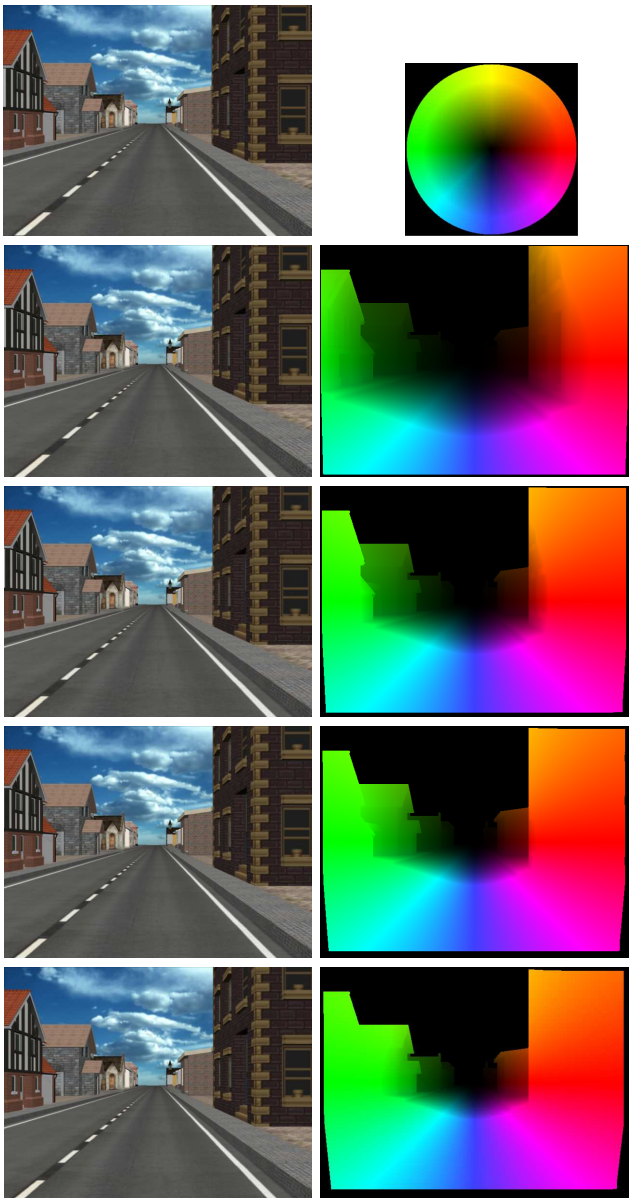

Fig. 2. Images from sequences of different speeds: $(top-left)$ first frame common for all sequences; $(top-right)$ colormap used to show the flow field; $(left-column)$ second frames from the sequences of different speeds S1, S2, S3 and S4 in the order from top to bottom; $(right-column)$ the ground-truth flow fields between the respective second frames and first frames.

V. EXPERIMENTAL ANALYSIS

Our aim is to find some relationship between the tuning of regularization terms in optical flow estimation and some feature of the given sequence, in particular the speed is considered as a representative feature. This relationship will

[1]www.autodesk.com/maya

allow an automatic update of regularization parameters according to the current speed of the vehicle. Here we consider the well known error measure Average Angular Error (AAE). The polar representation based optical flow computation is considered for analysis, which is the most suitable method for ADAS scenarios. We make use of the code provided by the authors of [18]. The polar optical flow method, as presented in section III, contains two regularization terms separately for two polar coordinate components: orientation and magnitude. The corresponding weighting parameters are α_θ and α_m. In this section, the two regularization terms are independently weighted and the AAEs are analyzed. We tried some values randomly and selected the values in the range 1, 2.5, 5, 10, 20, ..., 120 for both α_θ and α_m. Then, the optical flow is estimated for all the combinations of these values of α_θ and α_m, and the AAEs are computed. The optical flow fields are estimated for several frames in each sequence and the average of these AAEs in every sequence is used for comparisons. All the sequences start from a common position in the scene, so that the change in scene geometry should not affect the quality of the flow and thereby conclusions to be drawn. Figure 3 shows the 3D plot of AAEs obtained for sequence S1, when varying α_θ and α_m values. Similar AAE 3D plots can be obtained for all the sequences of different speeds. But, due to space limitations and for better comparabilities, 2D plots obtained by keeping one of the two regularization weights constant are shown. Figure 4 shows such plots of the errors (AAEs). There are six plots for few selected fixed α_θ values. Each plot contains four curves for four sequences of speeds S1, S2, S3 and S4. These curves indicate AAEs for different α_m values and for a fixed α_θ value. Similarly, Fig. 5 shows the error plots of the same four sequences for fixed α_m values but for varying α_θ.

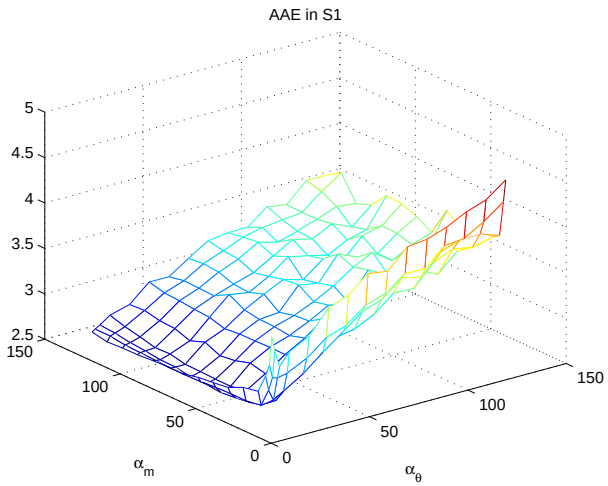

Fig. 3. 3D plot of AAEs from S1 for varying α_θ and α_m values.

From these plots it can be observed that for any combination of α_θ and α_m, the sequence S1 has higher AAE compared to sequences with higher speeds S2, S3, and S4. The minimum AAE value and the corresponding regularization weights for each of the sequences are given in Table I.

TABLE I

REGULARIZATION PARAMETER VALUES THOSE HAVE PRODUCED LEAST AAEs IN EACH OF THE SEQUENCES

Sequence	α_θ	α_m	AAE
S1	5	40	2.7266
S2	5	50	2.4437
S3	5	80	1.9024
S4	5	80	1.6627

TABLE II

REGULARIZATION PARAMETER VALUES THOSE HAVE PRODUCED LEAST AEPEs IN EACH OF THE SEQUENCES

Sequence	α_θ	α_m	AEPE
S1	10	20	0.0812
S2	10	30	0.1053
S3	10	60	0.1104
S4	10	50	0.1263

From this table one can re-affirm that the AAE decreases as the speed of the sequence increases. It can be observed in this table that the α_θ value keep constant (i.e., α_θ = 5 in all the cases). One can infer that, the α_θ value does not need to vary much according to the speed. We can also infer the same thing if we see the plots in Fig. 5. So α_θ needs to be fine tuned around this range and keep constant independently of the speed. If we see the α_m values in the table we can conclude that α_m should increase with the speed, for a constant α_θ. Looking at the plots in Fig. 4, we can observe that the α_m value needs to be tuned for a fixed value of α_θ.

We have also studied the properties of Average End Point Error (AEPE) similar to AAE for all the sequences and different values of α_θ and α_m. Table II shows the minimum AEPE for each sequence and the corresponding α_θ and α_m values. The same conclusion that we have drawn with respect to AAE can be drawn here also. Unlike with AAE, here the sequence with lowest speed S1 has got lesser AEPE compared to other sequences with higher speeds and the AEPE increases as the speed increases in the sequence. Since vectors in the flow field of the lowest speed (S1) are smaller in magnitude than in all the other cases, it is certain that the AEPE of S1 will be smaller compared with other sequences of higher speeds.

In order to check the effect of absence of either of the two regularization terms, we made either of the two parameters as zero. We found that making α_θ as zero and α_m as some positive value gives erroneous but visually appealing result. But if α_m as zero and α_θ as some positive value leads to the problem illposed. The flow fields are shown in Fig. 6. In conclusion, although polar representation seems to be the most appropriated way to tackle the optical flow estimation in ADAS domain, regularization terms are not equally significant. Results are less sensitive to the regularization term related with the orientation, while regularization term related to the magnitude seems more important in making

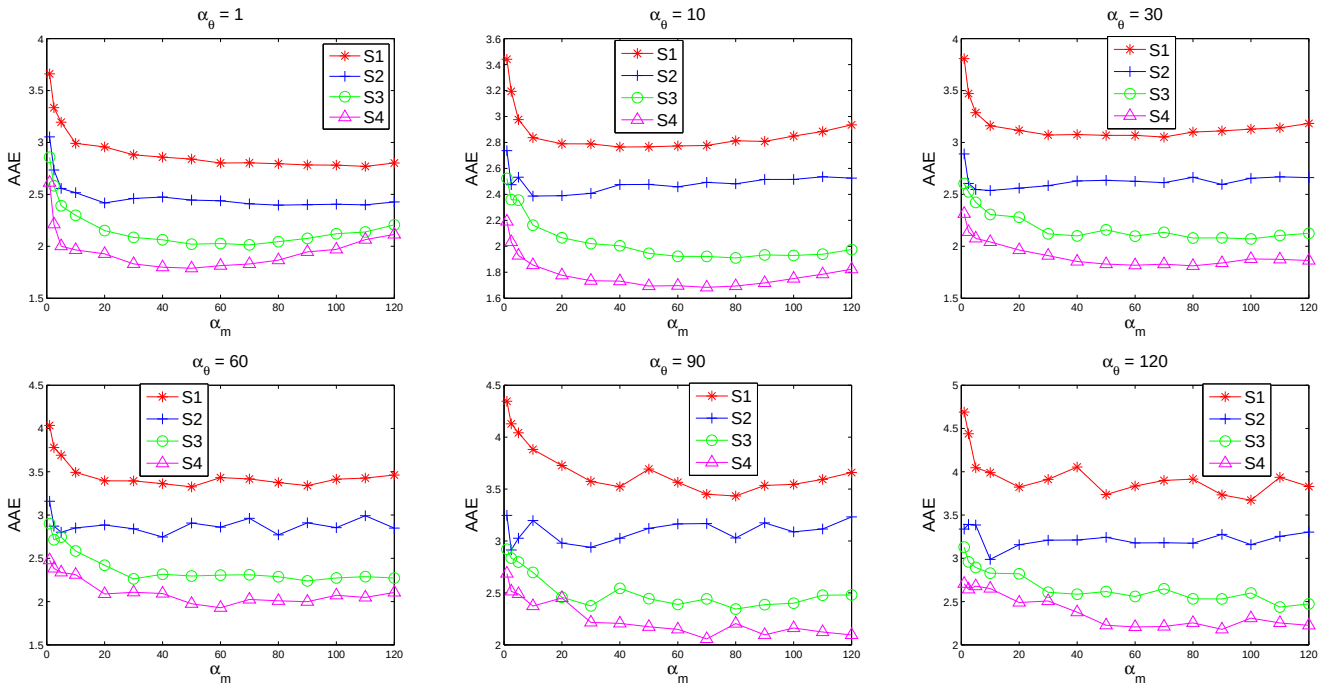

Fig. 4. Plots of AAEs, for few fixed α_θ values and for varying α_m values.

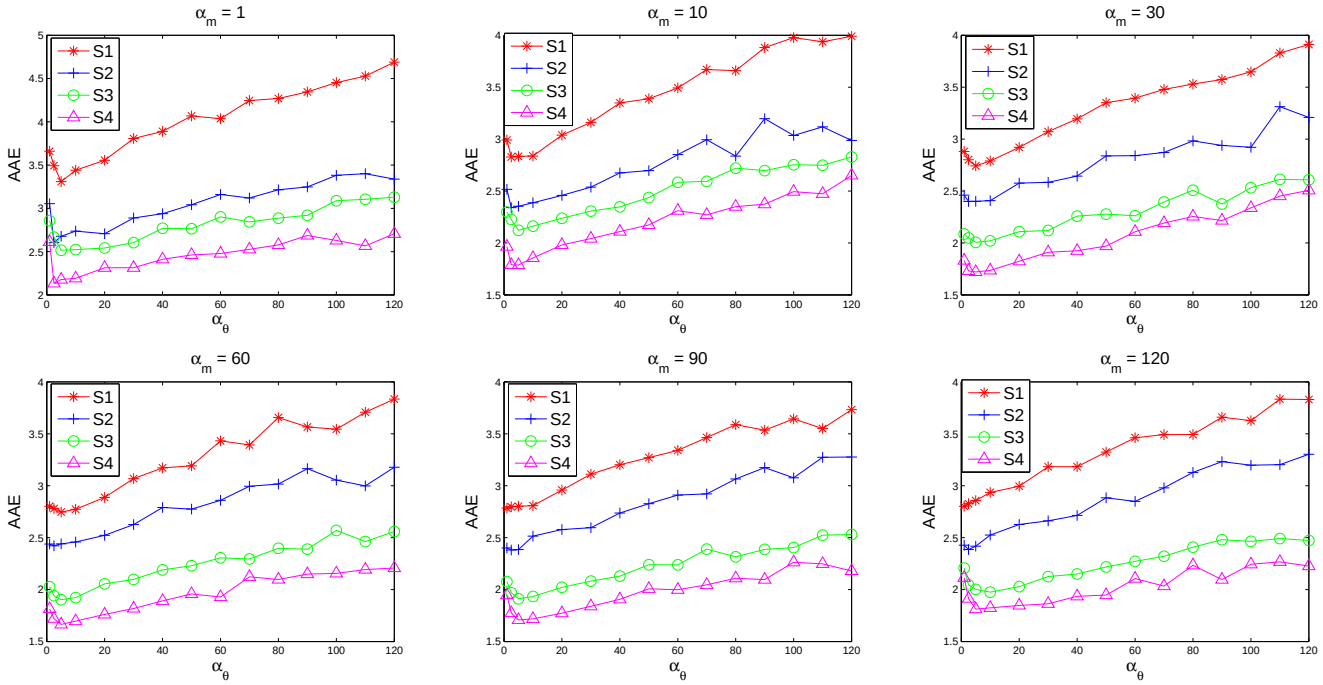

Fig. 5. Plots of AAEs, for few fixed α_m values and for varying α_θ values.

the problem well-posed and a more accurate optical flow estimation.

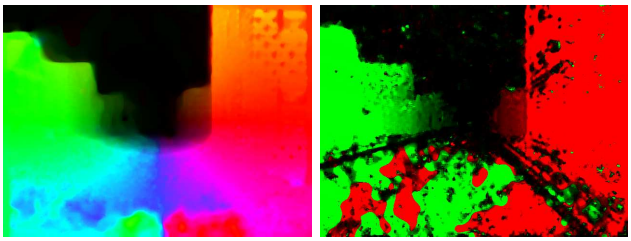

Fig. 6. $(left)$ Flow field when α_θ is zero. $(right)$ Flow field when α_m is zero.

VI. CONCLUSIONS

The current work explores the state of the art in optical flow estimation with the intention to assess their suitability for ADAS applications. Statistically it is evident that a polar representation of optical flow is better than the cartesian representation and is the most suitable one in driving scenarios. It is empirically concluded that the regularization term related to magnitude is more important compared to regularization term related to orientation. Further, it is evident that weighting of the regularization related to magnitude needs to be changed according to the speed of the vehicle, whereas the weight of the regularization term related to orientation can be kept at a constant smaller value. A new dataset for this empirical analysis is developed and can be obtained by contacting the authors. It consists of four image sequences of different speeds along with their ground-truth optical flow.

VII. ACKNOWLEDGMENTS

This work has been partially supported by the Spanish Government under Research Program Consolider Ingenio 2010: MIPRCV (CSD2007-00018) and Project TIN2011-25606. Naveen Onkarappa is supported by FI grant of AGAUR, Catalan Government. The authors would like to thank Oisin Mac Aodha for providing the Python code for raytracing with Maya.

REFERENCES

[1] B.K.P. Horn, B.G. Schunk: Determining optical flow. Artificial Intelligence, Vol. 17, 185-203, 1981.

[2] B.D. Lucas, T. Kanade: An iterative image registration technique with an application to stereo vision. In: DARPA Image Understanding Workshop, pp. 121–130, 1981.

[3] D. Sun, S. Roth, M.J. Black: Secrets of optical flow estimation and their principles. In: IEEE International Conference on Computer Vision and Pattern Recognition, pp. 2432–2439. San Francisco, CA, USA, 2010.

[4] J. L. Barron, D. J. Fleet, and S. S. Beauchemin: Performance of optical flow techniques, International Journal of Computer Vision, Vol. 12, No. 1, 43–77, 1994.

[5] A. Bruhn: Variational Optic Flow Computation- Accurate Modelling and Efficient Numerics, PhD Thesis, 2006.

[6] B. Galvin, B. Mccane, K. Novins, D. Mason, and S. Mills: Recovering motion fields-An evaluation of eight optical flow algorithms, In: British Machine Vision Conference. pp. 195-204, 1998.

[7] B. McCane, K. Novins, D. Crannitch and B. Galvin: On Benchmarking Optical Flow, Computer Vision and Image Understanding, Vol. 84, No. 1, 126-143, 2001.

[8] S. Baker, D. Scharstein, J. P. Lewis, S. Roth, M. J. Black, and R. Szeliski: A database and evaluation methodology for optical flow, In: IEEE International Conference on Computer Vision, pp. 1–8, 2007.

[9] A. Bruhn, J. Weickert, C. Schnrr: Lucas/Kanade Meets Horn/Schunck: Combining Local and Global Optic Flow Methods. International Journal of Computer Vision, Vol. 61, 211–231, 2005.

[10] S. Volz, A. Bruhn, L. Valgaerts, H. Zimmer: Modeling temporal coherence for optical flow. In: IEEE International Conference on Computer Vision, pp. 1116 - 1123, Barcelona, Spain, Nov. 6-13, 2011.

[11] J. Weickert, C. Schnrr: A theoretical framework for convex regularizers in PDE-based computation of image motion. International Journal of Computer Vision, Vol. 45, No. 3, 245-264, December 2001.

[12] Andreas Wedel, Daniel Cremers, Thomas Pock, Horst Bischof: Structure- and motion-adaptive regularization for high accuracy optic flow. In: IEEE International Conference on Computer Vision, pp. 1663–1668, 2009.

[13] Frank Steinbrcker, Thomas Pock, Daniel Cremers: Advanced Data Terms for Variational Optic Flow Estimation. Vision, Modelling and Visulaization Workshop, Braunschweig, Germany, pp. 155–164, 2009.

[14] Henning Zimmer, Andrs Bruhn, Joachim Weickert: Optic Flow in Harmony. International Journal of Computer Vision, Vol. 93, No. 3, 368-388, 2011.

[15] A. Wedel, T. Pock, C. Zach, H. Bischof, and D. Cremers: An improved algorithm for TV-L1 optical flow computation, In: Dagstuhl Visual Motion Analysis Workshop, 2008.

[16] T. Brox, A. Bruhn, N. Papenberg, and J. Weickert: High accuracy optical flow estimation based on a theory for warping, In: European Conference on Computer Vision, pp. 25-36, 2004.

[17] Yair Adato, Todd Zickler, Ohad Ben-Shahar: Toward robust estimation of specular flow, British Machine Vision Conference, pp. 22.1–22.11, 2010.

[18] Y. Adato, T. Zickler, and O. Ben-Shahar: A polar representation of motion and implications for optical flow , In: IEEE International Conference on Computer Vision and Pattern Recognition, pp. 1145–1152, Colorado Springs, USA, June, 2011.

[19] Stefan Roth and Michael J. Black: On the spatial statistics of optical flow. In: IEEE International Conference on Computer Vision, vol. 1, pp. 42–49, Oct. 2005.

[20] Oisin Mac Aodha, Gabriel J. Brostow, Marc Pollefeys: Segmenting video into classes of algorithm-suitability. In: IEEE International Conference on Computer Vision and Pattern Recognition, pp. 1054–1061, 2010.

[21] T. Vaudrey, C. Rabe, R. Klette, J. Milburn: Differences between stereo and motion behaviour on synthetic and real-world stereo sequences. In: Image and Vision Computing New Zealand, Christchurch, New Zealand, pp. 1-6, 2008.